THE ASTROPHYSICAL JOURNAL, 404:L63–L66, 1993 February 20

DISCOVERY OF A ROTATING PROTOPLANETARY GAS DISK AROUND THE YOUNG STAR GG TAURI

R. KAWABE,[1] M. ISHIGURO,[1] T. OMODAKA,[2] Y. KITAMURA,[3] AND S. M. MIYAMA[4]
Received 1992 July 20; accepted 1992 November 30

ABSTRACT

We have made aperture synthesis ^{12}CO($J = 1$–0) observations of a T Tauri star, GG Tau, in Taurus with 8″ resolution using the Nobeyama Millimeter Array (NMA). We have discovered a rotating gas disk having a radius of about 500 AU around GG Tau. The rotation velocity is 0.8 km s^{-1}/sin i at the radius, which is roughly consistent with a Kepler rotation around the central star. The inclination angle of the disk, i, is estimated to be about 60°, and the gas kinetic temperature is estimated to be about 8 K at that radius. The lower limit of the molecular gas mass in the disk is obtained to be 1.0×10^{-4} $M_\odot$ by assuming that the CO line is optically thin, and the upper limit is estimated to be about 0.4 $M_\odot$ from kinematical consideration. This would be the first example of the resolved protoplanetary gas disk with an AU scale of several 100.

Subject headings: ISM: molecules — planetary systems — stars: formation — stars: pre–main-sequence

1. INTRODUCTION

Various recent observations suggest that low-mass T Tauri stars have compact disks with radii of about 100 AU around the stars. *IRAS* observations revealed that T Tauri stars have far infrared excess (Rucinski 1985; Strom et al. 1988), and subsequent analysis of broad-band spectra from near-infrared to millimeter wavelengths suggest that the spectra are well consistent with the existence of a compact disk (Weintraub, Sandell, & Duncan 1989; Adams, Emerson, & Fuller 1990).

The cumulative observational evidence for the existence of the compact disks around T Tauri stars motivates observational studies which may shed light on the process of planet formation in protoplanetary disks (e.g., Beckwith et al. 1990; Omodaka, Kitamura, & Kawazoe 1992). An essential issue, not addressed to date, is the evolution of the gas component of these disks and the process of disk dispersal (e.g., Ohashi et al. 1991). Millimeter interferometric observations of HL Tau, T Tau, and DG Tau revealed gas disks around the stars (e.g., Sargent & Beckwith 1991). However, the size derived as about 4000 AU is much larger than those expected for compact circumstellar disks and the solar nebula. The observed gas around the three sources probably includes the gas in the envelope where stars were formed, as well as the gas in compact disks.

GG Tau is a T Tauri star in Taurus which radiates strong millimeter continuum dust emission at 1.3 mm. It is the second strongest source in the compilation according to Beckwith et al. (1990; $M_{\rm star} = 0.65\ M_\odot$, $L_{\rm IR} = 0.39\ L_\odot$, and age $= 3 \times 10^5$ yr). Ohashi et al. (1991) detected strong 3 mm continuum emission from GG Tau but could not detect significant CS($J = 2$–1) emission. Optical speckle interferometry suggests that GG Tau is a binary with a separation of 0.″255 under P.A. $= 9° \pm 2°$ (Leinert et al. 1991; another binary system, GG Tau/c, is located at about 10″ south of GG Tau). Recently, Skrutskie et al. (1993) discovered ^{12}CO emission toward GG Tau with the NRO 45 m telescope with a spatial resolution of 17″ (2400 AU assuming a distance to GG Tau of 140 pc). The observations showed a possible kinematic signature of a disk surrounding the star. However, the distribution and kinematics of the molecular gas have not been detected. We performed aperture synthesis ^{12}CO($J = 1$–0) observations of GG Tau which appears to be isolated from molecular clouds (Skrutskie et al. 1993) using the Nobeyama Millimeter Array (NMA) in order to investigate the distribution and kinematics of the molecular gas. Our observations revealed a rotating gas disk which may be a protoplanetary disk around GG Tau. In this *Letter*, we describe the physical nature of the disk and discuss the implications of our observations for the formation of a planetary system.

2. OBSERVATIONS

The ^{12}CO $J = 1$–0 and 115.27 GHz continuum emission from GG Tau were observed with the Nobeyama Millimeter Array on April 2 and May 2–4 in 1992. SIS receivers were used, and their system noise temperatures at the zenith were approximately 600 K in SSB (Kawabe et al. 1990). An FFT spectrocorrelator (FX) with 1024 velocity channels per baseline (Chikada et al. 1987) was used with a bandwidth of 320 MHz and a velocity resolution of 0.81 km s^{-1} for CO(1–0). Line-free channels were used for mapping continuum emission at 115 GHz (2.6 mm). The field center for the observations was at the position of GG Tau: R.A.(1950) = 04^{h}29^{m}37^s.2, decl.(1950) = 17°25′22.″0 (Rydgren et al. 1984), and the FOV is 65″.

Observations were made in two configurations over a span of 4 days. We obtained 20 baselines, with the minimum and maximum projected baseline lengths were 10 and 130 m, respectively. Therefore, our observations were insensitive to structures more extended than 45″. Bandpass and flux calibrations were carried out using the observations of 3C 273 and planets, respectively. Maps with 10″ × 6″ (P.A. = 138°) resolution for both the CO(1–0) and continuum emission were constructed using the CLEAN algorithm as provided by NRAO AIPS package. The absolute positional accuracy in the

[1] Nobeyama Radio Observatory, Nobeyama, Minamisaku, Nagano, 384-13, Japan. Nobeyama Radio Observatory (NRO) is a branch of the National Astronomical Observatory, the Ministry of Education, Science, and Culture of Japan.
[2] College of Liberal Arts, Kagoshima University, 1-21-30, Koorimoto, Kagoshima, 890, Japan.
[3] Department of Liberal Arts, School of Allied Medical Sciences, Kagoshima University, 8-35-1, Sakuragaoka, Kagoshima, 890, Japan.
[4] National Astronomical Observatory, 2-11-1, Oosawa, Mitaka, Tokyo, 181, Japan.

maps is estimated to be better than 2″, and the relative positional accuracy between CO(1–0) and the continuum maps is better than 0″.5. The uncertainty of their flux scale is 15%. The rms noise level in the continuum map was 11 mJy beam^{-1} and that in each CO(1–0) channel map with a 0.81 km s^{-1} width was 300 mJy beam^{-1} (corresponding to 0.46 K in brightness temperature, T_B).

3. RESULTS

3.1. CO(J = 1–0) *Emission*

Figure 1 shows velocity channel maps for velocities from V_{LSR} = 4.9 to 8.1 km s^{-1} over 3.2 km s^{-1} together with a map of dust continuum emission at 2.6 mm. Significant CO line emission was detected at the three velocity channels from V_{LSR} = 5.7 to 7.3 km s^{-1}; the emission at V_{LSR} = 4.9 km s^{-1} may also be real. There is no significant CO emission outside this velocity range. The peak line flux density in our 0.81 km s^{-1} resolution maps was 2.34 Jy beam^{-1} (3.6 K in T_B) at V_{LSR} = 5.7 km s^{-1}. The total flux density integrated over the above velocity range was 7.0 Jy km s^{-1}. The mean of V_{LSR} weighted by the CO emission is found to be 6.25 ± 0.1 km s^{-1}, and hereafter we assume that the systemic velocity of the CO emission associated with GG Tau is 6.3 km s^{-1} (this value is consistent with the systemic velocity determined from the NRO CO spectrum discussed in Skrutskie et al. 1993). Figure 1 shows that there exists a clear systematic velocity shift from 5.7 to 7.3 km s^{-1} along nearly the E-W direction (P.A. = 115°). The distribution of the CO emission at 6.5 km s^{-1} almost coincides with the dust continuum peak and is slightly elongated along the N-S direction. We could not detect significant CO emission toward the other member of the GG Tau system, GG Tau/c, although dust continuum emission has been detected (Simon & Guilloteau 1992) and N-S elongation of ^{13}CO(2–1) emission (including both GG Tau and GG Tau/c) has been suggested (Sargent et al. 1992).

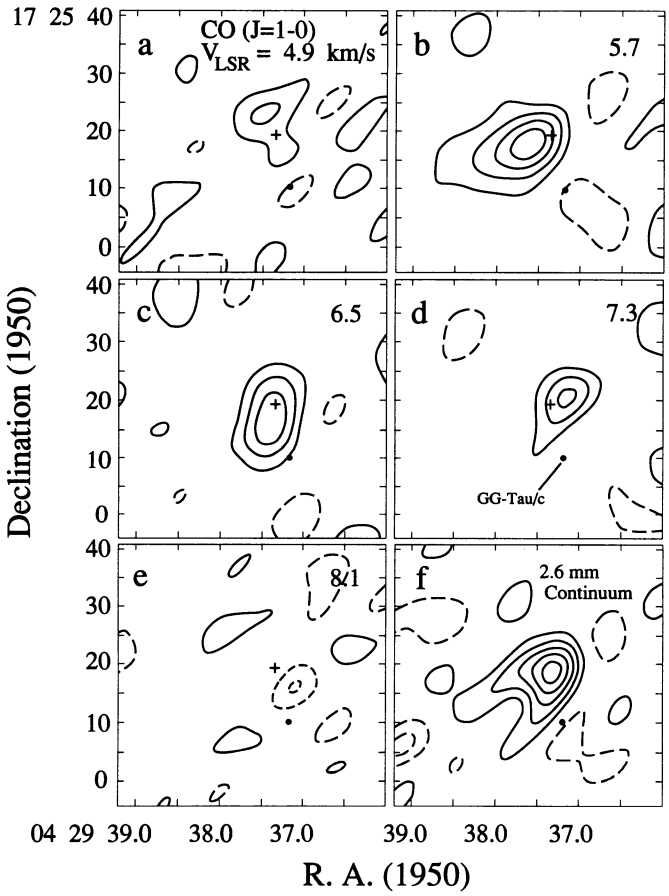

FIG. 1.—(*a*)–(*e*) Velocity channel maps for velocities from V_{LSR} = 4.9 to 8.1 km s^{-1} over 3.2 km s^{-1}. The center velocity of each channel with a 0.81 km s^{-1} width is shown in each panel. A cross indicates the peak position of 2.6 mm continuum emission (the position of GG Tau), and a dot indicates the position of GG Tau/c. The contour interval is 480 mJy beam^{-1} (1.5 σ). A contour with negative level is indicated with a broken line, and a zero-level contour is not shown. (*f*) Map of 2.6 mm continuum emission. The contour interval is 16.8 mJy beam^{-1} (1.5 σ).

Figure 2 shows maps of total CO intensity (Fig. 2*a*) integrated over three velocity channels (Figs. 1*b*–1*d*) and the overlay of the red- and blueshifted emission contours (Fig. 2*b*). The beam-deconvolved size of the molecular gas distribution in the total CO map is obtained to be 10″.6 ± 1″.0 × 5″.7 ± 0″.8 (P.A. = 125° ± 5°). The CO emission at 5.7 and 7.3 km s^{-1} is symmetrically located at each side of the centroid of dust continuum emission at 2.6 mm (star position) as shown in Figure 2*b*. The peaks of the red- and blueshifted emission shift by 3″.5 with respect to the centroid of the dust continuum emission. The two CO peaks define a position angle of about 115° ± 5°.

These observational results indicate that the molecular gas is arranged in a rotating gas disk centered at GG Tau. The disk is not perfectly edge-on because the CO emission at 6.5 km s^{-1} (nearly equal to the systemic velocity) extends roughly perpendicular to the direction of the E-W overall elongation. The shift of the blue- and redshifted components, 3″.5, from the continuum centroid corresponds to a projected radius of about 500 AU for the gas disk. Because of its compact scale, the disk may be considered as a protoplanetary disk (system). The NS elongation at 6.5 km s^{-1} is due to the CO emission originated from the near and far sides of the inclined disk which have nearly zero line-of-sight velocities. From the deconvolved size in the total CO intensity map, the inclination angle, i (i = 0° for face-on), of the disk is estimated to be $\cos^{-1}$ (5″.7/10″.6) = 57°.

The blue CO emission at 5.7 km s^{-1} is spatially resolved by the synthesized beam, though the red CO emission at 7.3 km s^{-1} is almost pointlike. This may be due to asymmetry of the velocity channels with respect to the actual systemic velocity, 6.3 km s^{-1}; the two blue and red channels are shifted by 0.6 and 1.0 km s^{-1} from the systemic velocity, respectively. The beam deconvolved size of the blue component is as large as 11″.6 × 5″ and has a P.A. of 108°. The position angle is just coincident with that between the two peaks of red and blue components, 115°. This indicates that the protoplanetary disk extends over $r \geq$ 500 AU at the east side.

3.2. *Continuum Emission*

Figure 1*f* shows a map of the continuum emission at 115.27 GHz, although its distribution was not resolved in our observations. The total flux density at 115.27 GHz is found to be 96 ± 15 mJy, which is consistent with that at 110 GHz, 80 ± 5 mJy (Beckwith et al. 1990) and that at 98 GHz, 41 ± 4 mJy (Ohashi et al. 1991) assuming a 15% flux uncertainty and a spectral index of nearly 3–4. The continuum emission, as evaluated from a two-dimensional Gaussian fit to the map, is centered at R.A.(1950) = 04^{h}29^{m}37^s.34, decl.(1950) = 17°25′19″.5. The position is shifted from the stellar position listed by Rydgren et al. (1984) by about 2″–3″, which we believe to be consistent with the uncertainties of absolute positions included in both the data. We identify the 2.6 mm continuum

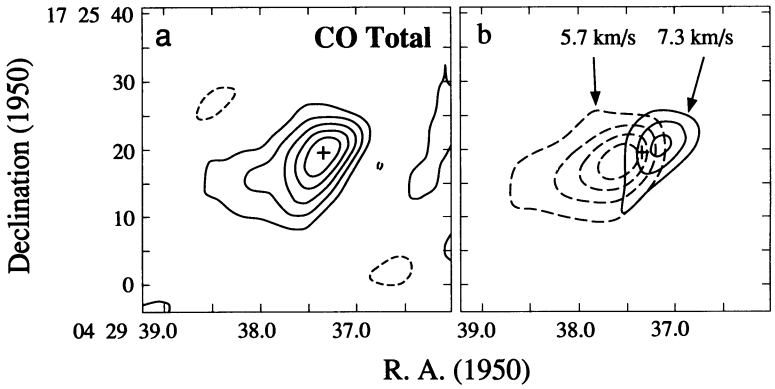

FIG. 2.—(*a*) Map of total CO intensity integrated over three velocity channels (Figs. 1*b*–1*d*). The contour interval of the total CO map is 270 mJy beam^{-1} (1.5 σ). (*b*) Red (*solid*) and blueshifted (*broken*) CO components in Figs. 1*b* and 1*d*.

position with a position of the star because the relative positional accuracy between the CO and continuum maps ($\leq 0''.5$) is much better than the absolute positional accuracy ($\leq 2''$).

4. DISCUSSION

First, we summarize the physical parameters of the protoplanetary gaseous disk around GG Tau based on our observational results and estimate the disk mass. The radius of the disk is roughly estimated to be 500 AU from the separation of the two peaks of the blue- and redshifted CO emissions. In addition, the rotation velocity at $r = 500$ AU is estimated to be (0.6–1.0)/sin i km s^{-1} from the observed velocities of the two peaks (0.6 and 1.0 km s^{-1} for the blue and red components, respectively) relative to the assumed systemic velocity, 6.3 km s^{-1}.

The inclination angle of the disk is about 57° as noted in the previous section. The position angle of the major axis of the disk is estimated to be around 120° from the orientation of two peaks and the elongation of the beam deconvolved size in the total CO map. The gas kinetic (excitation) temperature at $r = 500$ AU was estimated to be about 8 K for the east side of the disk using the beam deconvolved brightness temperature of the CO emission. The derived temperature is roughly consistent with that expected from a radial temperature gradient of $r^{-1/2}$, with a temperature of 180 K at 1 AU (Beckwith et al. 1990).

The mass of protoplanetary nebulae is a very critical parameter in order to understand the formation scenario of planetary systems. In proposed theoretical models of the solar nebula (e.g., Hayashi, Nakazawa, & Nakagawa 1985), there are two types of nebula assumed; one is a low-mass (0.01 $M_\odot$) nebula and another is a high-mass (1 $M_\odot$) nebula. A lower limit of H_2 mass is estimated to be 0.0001 $M_\odot$ from the observed CO total flux, assuming the galactic CO abundance ($CO/H_2 = 9 \times 10^{-5}$), T_{EX} of 10 K, and an optically thin case. However, gaseous CO molecules will be converted to solid CO for temperatures lower than 13–16 K, ignoring evaporation from dust surface [for a wide H_2 density range of $n(H_2) = 10^4$–10^{10} cm^{-3}; Umebayashi 1992]. In the "outer" and cold region of the disk ($r = 500$ AU), almost all of the CO might be in solid form. Observations of solid CO absorption at near-infrared wavelengths may provide independent evidence regarding the presence or absence of solid CO.

We can estimate the mass of the protoplanetary gas disk from the following kinematical consideration using the estimated radius and rotation velocity. We can plot the line-of-sight velocity at $r = 500$ AU in the mass-inclination space as shown in Figure 3. The mass in Figure 3 is a total (star + gas) mass inside a radius of 500 AU and should be higher than the mass of the central star, 0.65 $M_\odot$ (estimated for "single" star; Strom et al. 1989; Beckwith et al. 1990). The line-of-sight velocity at $r = 500$ AU is found to be in the range from 0.6 to 1.0 km s^{-1} based on our results, and is indicated by the hatched region. The range of the inclination angle is 57° ± 10°. These restrictions specify an allowed region as shown in Figure 3, which roughly gives us kinematical upper limits of the total system mass and gas mass, 1.05 and 0.4 $M_\odot$, respectively. It should be noted that we neglected to subtract the mass of the secondary because there is no reliable estimate of the mass, and that the gas mass would, however, be a safe upper boundary of the disk mass. The upper limit of the gas mass is consistent with the H_2 mass, 0.14 $M_\odot$ (Ohashi et al. 1991) and 0.29 $M_\odot$ (Beckwith et al. 1990) estimated from the recent observations of dust continuum emission from GG Tau.

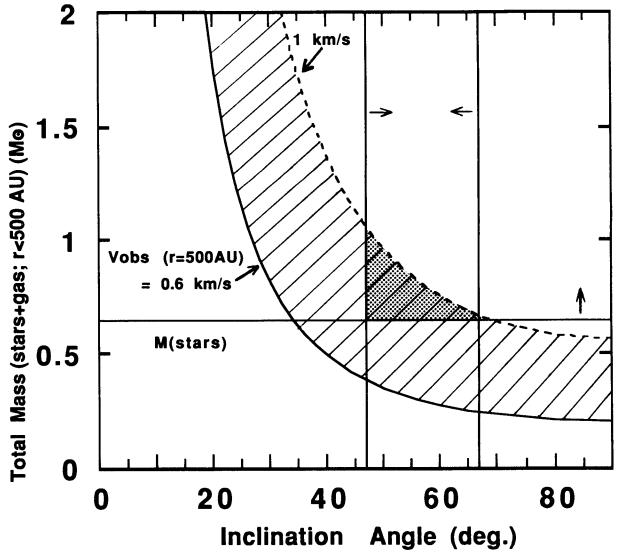

FIG. 3.—Plot of the line-of-sight rotation velocity at $r = 500$ AU in the mass-inclination space. The mass is a total (star + gas) mass inside a radius of 500 AU and should be higher than the mass of the central star, 0.65 $M_\odot$ (Beckwith et al. 1990). The observed line-of-sight velocity ranges from 0.6 to 1.0 km s^{-1} and is indicated by the hatched region. The range of the estimated inclination angle is also shown. The allowed region in the space is indicated by a shaded region.

The physical parameters of the disk are summarized in Table 1 with the parameters of GG Tau. Our results are consistent with the elongated structure of dust emission in GG Tau (P.A. $\sim 150°$) found by the IRAM interferometer (Simon & Guilloteau 1992). The elongated structure would be corresponding to the central part of the protoplanetary gas disk. Our derived disk parameters also agree with the results from the extensive modeling which is based on data with the 45 m telescope (Skrutskie et al. 1993).

Next, we discuss the gravitational stability of the protoplanetary disk we discovered. From the age of the GG Tau (Beckwith et al. 1990), the age of the disk must be less than 3×10^5 yr. If this disk were gravitationally unstable, its gas would be dispersed in several dynamical times by gravitational torque arising from nonaxisymmetric modes. The dynamical time is estimated to be of the order of the Kepler time at the outer disk edge (500 AU) and it is about 10^4 yr, much shorter than the disk age. In order that the disk exists for such a time as long as 10^5 yr, it must be stable against gravitational instability. We can now estimate the upper limit of the disk mass for a stable disk. We assume that the rotation law is Keplerian, the surface density of the disk is $\Sigma = \Sigma_0(r/r_0)^{-p}$ and the temperature is $T = T_0(r/r_0)^{-q}$, where Σ_0, T_0, r_0, p, and q are constants. The disk mass (M_d) is calculated as $M_d \simeq [2\pi\Sigma_0 r_0^2/(2 - p)](r_{\rm out}/r_0)^{2-p}$ if $r_{\rm out} \gg r_{\rm in}$ and $p < 2$, where $r_{\rm out}$ and $r_{\rm in}$ are the disk radii at the outer and inner edges, respectively. For disk stability we assume that the value of Toomre's Q ($Q = c_s\Omega/\pi G\Sigma$) must be greater than a critical value, $Q_{\rm critical} \sim 3$ (Binney & Tremaine 1987; Adams, Ruden, & Shu 1989). Under these assumptions, the upper limit of the disk mass is $0.175\ M_\odot (3/Q_{\rm critical})(T_0/300\ {\rm K})^{1/2}(M_*/0.65\ M_\odot)^{1/2}$, where we assume $p = 3/2$, $q = 1/2$, and $r_{\rm out} = 500$ AU. This upper limit is quite consistent with the upper limit obtained by our observation.

As noted, recent IR-speckle observations (Leinert et al. 1991) revealed that GG Tau has a companion at an angular distance of $0''.255 \pm 0''.01$ at P.A. $= 9° \pm 2°$. The projected separation is about 38 AU. If the disk and this companion have the same origin, the companion should lie along the disk plane. From the position angle of the disk and the companion along with the inclination angle obtained in the previous subsection, the true separation of the GG Tau binary components would be about 70 AU. Since the disk size is estimated to be 500 AU, it must be an external accretion (excretion) disk, i.e., binary plus a surrounding common disk (Pringle 1991; Artymowicz et al. 1991). In this case, the radius of the outer disk edge continues to grow as a result of perturbations induced by binary rotation. This may be one factor contributing to the disk size. As for the inner edge, the gas would be cleaned out by the binary motion until the radius of their outer Lagrange point at least. They would be of the order of 100 AU. On the other hand, since there is a substantial near IR excess with some amount (Rucinski 1985), each companion probably has a small size disk with a radius of about 10 AU. Consequently, this system may have a double structure, i.e., two accretion disks and an external excretion disk.

TABLE 1

PARAMETERS OF GG TAURI AND THE GAS DISK IN GG TAURI

Parameter	Value
$M_{\rm star}$[a]	$0.65\ M_\odot$
$L_{\rm IR}$[a]	$0.39\ L_\odot$
$L_{\rm tot}$[a]	$0.03\ L_\odot$
Age[a]	3×10^5 yr
r	500 AU
$v_{\rm rot}$	(0.6–1.0)/sin i km s^{-1} at $r = 500$ AU
i	$57° \pm 10°$ ($i = 0°$ for face-on)
P.A.	$120° \pm 10°$ (disk major axis)
T	8 K at $r = 500$ AU
$M(H_2)$	$\geq 0.0001\ M_\odot$ (from total CO Flux)
$M(H_2)$	$\leq 0.4\ M_\odot$ (from kinematical consideration)
$M(H_2)$	$\leq 0.18\ M_\odot$ (from disk instability)
$M(H_2)$[a]	$0.29\ M_\odot$ (from 1.3 mm dust emission)
$M(H_2)$[b]	$0.14\ M_\odot$ (from 3 mm dust emission)

[a] From Beckwith et al. 1990.
[b] From Ohashi et al. 1991.

We thank the staff in the Nobeyama Radio Observatory for operation of the Nobeyama Millimeter Array. We also thank Professor Y. Kozai for his critical reading of this manuscript and for continuous encouragement and thank Professors S. E. Strom and K. M. Strom for useful discussions.

REFERENCES

Adams, F. C., Emerson, J. P., & Fuller, G. A. 1990, ApJ, 357, 606
Adams, F. C., Ruden, S. P., & Shu, F. H. 1989, ApJ, 347, 959
Artymowicz, P., Clark, C. J., Lubow, S. H., & Pringle, J. E. 1991, ApJ, 370, L35
Beckwith, S. V. W., Sargent, A. I., Chini, R. S., & Güsten, R. 1990, AJ, 99, 924
Binney, J., & Tremaine, S. 1987, Galactic Dynamics (Princeton: Princeton Univ. Press)
Chikada, Y., et al. 1987, Proc. IEEE, 75(9), 1203
Hayashi, C., Nakazawa, K., & Nakagawa, Y. 1985, in Protostars and Planets II, ed. D. C. Black & M. S. Matthews (Tucson: Univ. of Arizona Press), 1100
Kawabe, R., Inatani, J., Kasuga, T., Ishiguro, M., Yamamoto, M., Yamaji, K., & Watasawa, K. 1990, in Proc. of the 3rd Asia-Pacific Microwave Conference, 217
Leinert, Ch., Haas, M., Richichi, A., Zinnecker, H., & Mundt, R. 1991, A&A, 250, 407
Ohashi, N., Kawabe, R., Hayashi, M., & Ishiguro, M. 1991, AJ, 102, 2054
Omodaka, T., Kitamura, Y., & Kawazoe, E. 1992, ApJ, 396, L87
Pringle, J. E. 1991, MNRAS, 248, 754
Rucinski, S. M. 1985, AJ, 90, 2321
Rydgren, A. E., Schmelz, J. T., Zak, D. S., & Vrba, F. J. 1984, Publ. US Naval Obs., 25, 1
Sargent, A. I., et al. 1992, private communication
Sargent, A. I., & Beckwith, S. 1991, ApJ, 382, L31
Simon, M., & Guilloteau, S. 1992, ApJ, 397, L47
Skrutskie, M. F., et al. 1993, ApJ, in press
Strom, K. M., Strom, S. E., Edwards, S., Cabrit, S., & Skrutskie, M. F. 1989, AJ, 97, 1451
Strom, K. M., Strom, S. E., Kenyon, S. J., & Hartmann, L. 1988, AJ, 95, 534
Umebayashi, T. 1992, private communication
Weintraub, D. A., Sandell, G., & Duncan, W. D. 1989, ApJ, 340, L69